The Astrophysical Journal Supplement Series, 218:19 (9pp), 2015 June doi:10.1088/0067-0049/218/2/19

OPTIMIZATION OF A SOLAR SIMULATOR FOR PLANETARY-PHOTOCHEMICAL STUDIES

Et-touhami Es-sebbar[1,2], Yves Bénilan[1], Nicolas Fray[1], Hervé Cottin[1], Antoine Jolly[1], and Marie-Claire Gazeau[1]
[1] Laboratoire Interuniversitaire des Systèmes Atmosphériques, LISA, UMR 7583, CNRS, Université Paris Est Créteil and Université Paris Diderot, Institute Pierre Simon Laplace, 61 Avenue du Général De Gaulle, F-94010 Créteil Cedex, France
[2] Laboratoire de Physique des Gaz et des Plasmas (LPGP), UMR 8578, CNRS, Université Paris-Sud, Bât 210, F-91405 Orsay Cedex, France; ettouhamiessbbar@gmail.com
Received 2015 March 7; accepted 2015 April 23; published 2015 June 5

ABSTRACT

Low-temperature microwave-powered plasma based on hydrogen and hydrogen with noble gas mixtures are widely used as a continuous vacuum ultraviolet (VUV) source in laboratory experiments carried out to mimic the photochemistry in astrophysical environments. In this work, we present a study dedicated to optimizing such sources in terms of mono-chromaticity at Lyα (H(Lyα) line at 121.6 nm $\sim$ 10.2 eV) and high spectral irradiance. We report the influence on the emission spectrum of a wide range of experimental conditions including gas composition (pure H_2, pure He, and H_2/He mixture), gas pressure, flow rates, and microwave power. The absolute spectral irradiance delivered by this VUV light source has been measured. With a microwave input power of 100 W, the best conditions for producing a quasi-monochromatic source are a 1% H_2/He gas mixture at a total pressure of 5 mbar and a flow rate of 2 sccm. By changing the microwave input power from 30 to 120 W, H(Lyα) increases by more than one order of magnitude. A comparison between the current measurements and the solar VUV spectral irradiance is reported over 115–170 nm.

Key words: astrochemistry – plasmas – Sun: UV radiation – techniques: spectroscopic

1. INTRODUCTION

Vacuum ultraviolet (VUV) light is one of the main energetic sources driving chemical evolution occurring in planetary atmospheres and in the interstellar medium (ISM; Weber & Greenberg 1985; Ehrenfreund et al. 1997; Gazeau et al. 2007; Muñoz Caro & Schutte 2003; Ferris et al. 2005; Tran et al. 2008). Laboratory simulations of most astrophysical environments require representative VUV sources, particularly in terms of wavelength dependence and spectral irradiance. Since the 1960s (Warneck 1962; Okabe 1964; Samson 1967; Davis & Braun 1968), microwave-powered hydrogen plasmas are frequently used in laboratory experiments to simulate the energy deposition of stellar photons at the top of planetary atmospheres or in the ISM. Microwave plasma sources are simple, quite stable, and low cost. Their optically active medium can be large (up to several centimeters), and they can easily be implemented to different experimental setups. However, microwave-powered plasmas are generally not well defined since the emission spectrum depends on numerous experimental parameters (Masoud et al. 2004; Chen et al. 2014). The general assumption is that hydrogen plasmas simulate the solar irradiance spectrum (Truillier et al. 2004; Figure 1), which is dominated by the atomic hydrogen Lyα line (H(Lyα)) at 121.6 nm, but this is not necessarily true. As shown by Cottin et al. (2003), the H(Lyα) emission could account for only 5% of the total VUV emission intensity between 100 and 200 nm. More recently, Chen et al. (2014) have shown that the contribution of H(Lyα) could range from 0% to 80% of the emission in the 115–180 nm range depending on the operating experimental conditions. Apart from the H (Lyα) line, the other intense emissions generally observed are located around 160 nm and are attributed to the Lyman band ($B^1\Sigma_u - X^1\Sigma_g$) of molecular H_2. We decided to record the VUV emission spectrum of microwave-powered plasma lamps with pure H_2, pure He, and H_2/He gas mixtures and to study the influence of several parameters such as microwave power, gas pressure, and flow rate. Such studies have already been reported by Fozza et al. (1998) for H_2 and H_2/Ar as well as O_2 and O_2/Ar, by Masoud et al. (2004) for H_2/Ne, and by Chen et al. (2014) for H_2 and H_2/He. However, to our knowledge, Jenniskens et al. (1993) and Cruz-Diaz et al. (2014) are the only two references that compare the spectral irradiance of a microwave-powered hydrogen lamp with a natural astrophysical light source (i.e., the diffuse medium interstellar and dense molecular cloud radiation field within the 90–260 nm range). Interpretations of laboratory simulations depend on quantitative values in order to be compared with theoretical and/or observational data. To provide meaningful information, the spectral irradiance of the VUV sources used in the laboratory has to be accurately compared with the VUV field present in astrophysical environment. In this paper, we present a detailed description of our experimental setup and the results leading to the choice of an accurate solar simulator in terms of spectral irradiance to be useful for photochemical studies. To further characterize our microwave discharge plasma, we have also measured the absolute spectral irradiance over the 115–170 nm range using the chemical actinometric method.

2. EXPERIMENTAL SETUP

The experimental setup is shown in Figure 2. The plasma is produced in a quartz tube (8 mm internal diameter, 10 mm external diameter, and 20 cm length) in which H_2, He, or H_2/He mixture are introduced. The discharge is excited using a McCarrol cavity (Opthos Instruments, Inc.) connected to a 2.45 GHz microwave generator (SAIREM) with a maximum output of 300 W. The discharge tube is cooled by air flow to keep a constant temperature. The gas flow rate can be fixed and controlled by two mass flow controllers (MKS 1179B): one between 0.2 and 76 sccm (standard $cm^3\ min^{-1}$) for He and one between 0.2 and 6 sccm for H_2. In the case of H_2/He mixtures, changing the flow rates of both gases varies the percentage of H_2 in He. The gas pressure, ranging from 0.7 to 80 mbar, is

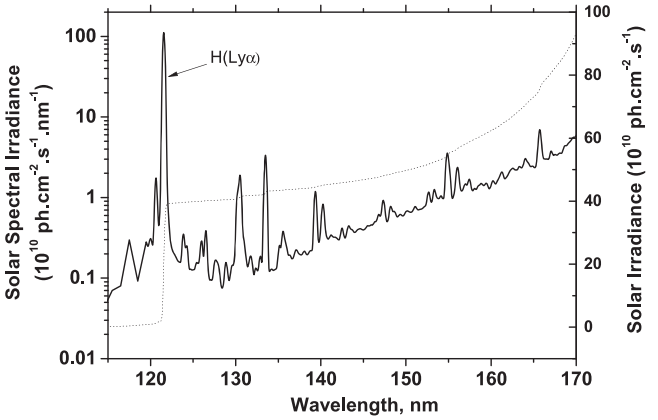

Figure 1. Solar spectral irradiance received at the top of the Earth's atmosphere (ATLAS 3 spectrum of Thuillier et al. 2004; left scale, full line) and integrated solar irradiance starting from 115 nm (right scale, dashed line).

measured using an MKS pressure gauge (model MKS 722A). Before starting measurements and allowing gas flow, the plasma tube is evacuated through a turbo-molecular pump backed by a rotary mechanical pump to reach a vacuum of about 10^{-6} mbar. Since the VUV emission decreases at higher pressures, flow rates are limited to 76 sccm.

The VUV emission spectrum from the microwave-powered plasma is recorded between 115 and 170 nm using a VUV spectrometer (Horiba-Jobin-Yvon, H20-UVL) placed longitudinally to the discharge tube. The spectrometer is isolated from the plasma source by a MgF_2 window with a cutoff around 115 nm and pumped by a turbo-molecular pump to keep a pressure of about 10^{-7} mbar. The VUV light is collimated with a concave mirror, directed to a 1200 g mm^{-1} grating, and recorded by a VUV photomultiplier tube (Hamamatsu R-8486). The VUV emission is focalized on the entrance slit situated at a distance of 20 cm from the center of the discharge. A computer controls scanning and acquisition of the data. All spectra are recorded with a spectral resolution of 0.06 nm and a scan rate of 0.3 nm s^{-1}. Transmission decrease has been observed during the experimentations requiring frequent cleaning of the MgF_2 window.

In addition to the VUV apparatus described above, a Fourier transform infrared (FTIR) spectrometer (Bruker Equinox 55) is used to monitor the CO infrared band during the actinometry experiments. Details of the setup can be found elsewhere (Romanzin et al. 2010). In short, the microwave discharge plasma light source is connected to a multi-reflection white-cell containing CO_2. Some CO is produced by the CO_2 photolysis, and its absorbance is followed by infrared spectroscopy. Each infrared spectrum being averaged over 10 minutes, the spectral resolution is 0.5 cm^{-1}.

3. RESULTS

3.1. Influence of Plasma Parameters on the VUV Emission Spectrum

3.1.1. VUV Spectra in Pure H_2, He, and 1% H_2/He Mixture

VUV spectra from microwave discharge with pure H_2, pure He, and a mixture of 1% H_2/He are shown in Figures 3(a)–(c), respectively. Results are presented to illustrate VUV emissions between 115 and 200 nm. The observed atomic lines and molecular bands are labeled in Table 1. The spectrum of pure H_2discharge (Figure 3(a)) has two characteristic features: (i) a weak line near 121.6 nm due to atomic H (Lyα) and (ii) a large band emission between 150 and 170 nm due to the Lyman band of molecular H_2 ($B^1\Sigma_u - X^1\Sigma_g$).

In pure He (Figure 3(b)), the VUV spectrum is strongly dominated by atomic lines of H(Lyα) and N I emissions at 149.4 and 174.5 nm. The molecular band ($B^1\Sigma_u - X^1\Sigma_g$) of $H_2$is also observed, but its contribution is smaller compared to pure H_2 (Figure 3(a)) or 1% H_2/He (Figure 3(c)). Other atomic lines of N I (119.9 and 124.3 nm) and O I (130.5 nm) are also identified in the spectrum as well as C I lines at 165.7 and 193.1 nm. The emissions of H, C, N, and O lines in pure He plasma can be explained by the presence of trace impurities in the He gas cylinder and/or by small air leaks in our experiments. The observed atomic lines are similar to those seen by Kurunczi et al. (2001) using high-pressure micro-hollow discharge in He. Emission of H(Lyα) is also observed in pure He by Fuchs et al. (1995) using a low-frequency He discharge lamp and by Morozov et al. (2008) in pure Ne. Aside from the intense H(Lyα) emission, Fedenev et al. (2004) have observed the nitrogen lines from a radiation source using pure He excited by an electron beam. The emission of those atomic lines in pure rare gas discharges is due to the role played by metastable species such as He* and He_2* that can efficiently transfer their energy to molecular and atomic species (Motret et al. 1985; Kurunczi et al. 2001; Rahman et al. 2004).

Figure 3(c) illustrates the main spectral features using the microwave plasma with 1% H_2/He. The emission spectrum is similar to that obtained in pure $H_2$with the H(Lyα) line and H_2molecular bands. However, the contribution of the H(Lyα) line to the overall spectra is enhanced while the H_2 band is reduced compared to the pure H_2 spectrum. Weak atomic lines of O I (130.5 nm), N I (149.4 and 174.5 nm), and C I (193.1 nm) are also observed. Note that N I, O I, and C I lines are not observed in the pure H_2 spectrum because of the absence of energy transfer by metastable He* and He_2* (Figure 3(a)). The role of metastable He* and He_2* is particularly evident for the increase of the H(Lyα) line (Motret et al. 1985; Kurunczi et al. 2001; Rahman et al. 2004).

As already observed by Warneck (1962), Davis & Braun (1968), Chen et al. (2011), Cook et al. (2014), and Chen et al. (2014), it turns out that the mixture of H_2 with He seems to be the best alternative to obtain a spectrum dominated by the H (Lyα) line needed to reproduce the solar spectrum. In the following, mixtures of H_2 in He will be further characterized by testing the effect of the percentage of H_2 in He, the total pressure (p), the flow rate (Q), and finally the (Q/p) ratio on the VUV emission spectrum.

3.1.2. Effect of H_2 Addition in He

VUV emission spectra from H_2/He microwave plasma have been recorded with various percentages of H_2 in He. The amount of H_2 has been determined by setting the flow rates of both gases; the total pressure and the microwave input power have been kept constant at 4.7 mbar and 100 W, respectively. The values of the ratio between the flow rate and the pressure, noted as (Q/p) here, were kept in the asymptotic high residence time regime (see Section 3.1.4). Figure 4(a) shows that the H (Lyα) emission integrated between 120 and 124 nm varies with the percentage of H_2 added in He, and it reaches a maximum at around 1%. In the case of 10% H_2 in He, the integrated value has decreased by a factor of three compared to the peak value at

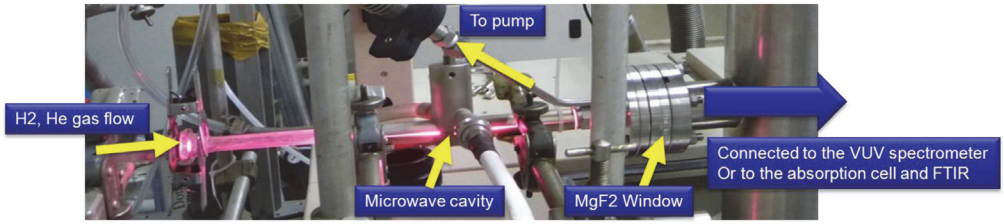

Figure 2. Experimental setup of H_2/He microwave plasma.

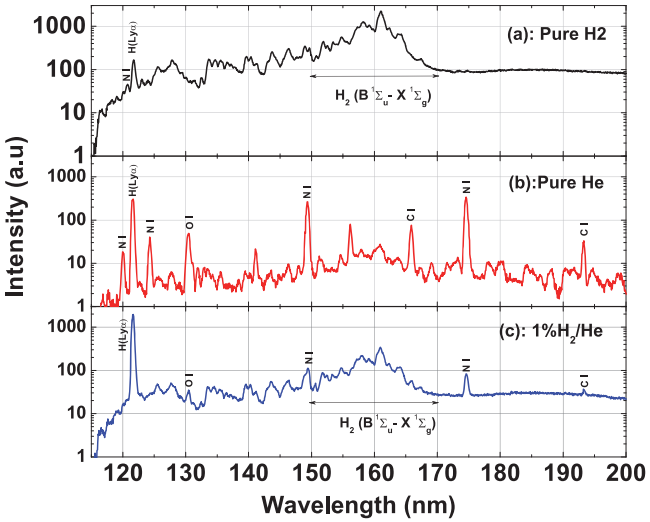

Figure 3. VUV emissions from microwave plasma with (a) pure H_2, (b) pure He, and (c) 1% H_2/He mixture. Flow rates are (a) 5.78 sccm, (b) 76 sccm, and (c) 0.7/70 sccm for H_2/He. For all measurements, the mean discharge power is 100 W, and the gas pressure is 4.7 mbar.

Table 1
Summary of the Observed Atomic Lines and Molecular Band from Pure H_2, Pure He, and 1% H_2/He Microwave Plasma Source

Identified Species	Wavelength (nm)	Transition
N I	119.9	$2p^3 {}^4S^0$–3 s ^4P
H I	121.6	2 p $^2P_0$–1 s ^2S
N I	124.3	$2p^3 {}^2D^0$–3 s ^2D
O I	130.5	$2p^4 {}^3P$–3 s $^3S^0$
N I	149.4	$2p^3 {}^2D^0$–3 s ^2P
C I	165.7	$2p^2 {}^3P$–3 s $^3P^0$
N I	174.5	$2p^3 {}^2P^0$–3 s ^2P
C I	193.1	$2p^2$ ^{1}D–3 s $^1P^0$
$H_2(B^1\sum_u - X^1\sum_g)$	150–170	$B^1\sum_u - X^1\sum_g$

Note. See Figure 3 for experimental conditions.

1% of H_2. However, Figure 4(a) also shows that the integrated emission between 115 and 170 nm increases continuously with the percentage of H_2 in He. Then, the contribution of the H (Lyα) line emission to the overall spectrum can be calculated by dividing the integrated flux between 120 and 124 nm to the integrated flux between 115 and 170 nm. As shown in Figure 4(b), the contribution of H(Lyα) line intensity relative to the overall spectrum increases to reach a maximum of about 32% for (0.25 ± 0.05)% of H_2 in He and then decreases below 10% when the amount of H_2 in He exceeds 4%. The rise of H (Lyα) line intensity is related to an increase in H atoms since H_2 concentrations in He increase. However, the emission of H (Lyα) in H_2/He mixture is strongly related to the quenching process with He. When the quenching exceeds the production of H atoms, H(Lyα) emission drops (Masoud et al. 2004). Self-absorption and trapping of the H(Lyα) can also contribute to reducing the emission at high H_2 concentration in He (Masoud et al. 2004). In conclusion, while the overall integrated intensity increases with the percentage of H_2 in He, the H(Lyα) maximum intensity is obtained for 1% of H_2 in He and the maximum contribution of H(Lyα) relative to the overall intensity is observed for even lower percentages. Therefore a percentage as low as 0.25% H_2 in He would optimize the contribution of H(Lyα) to the overall emission of our VUV lamp in the present operating conditions (4.7 mbar, 100 W).

3.1.3. Influence of the Pressure

To study the influence of the gas pressure, we have considered a mixture of 1% H_2/He and an unchanged discharge power of 100 W. We focused our attention on the contribution of H(Lyα) relative to the overall emission (i.e., between 115 and 170 nm). As can be seen from Figure 5(a), the integrated emission of H(Lyα) slightly increases by about 16% from low pressures up to about 10 mbar and then decreases considerably for higher pressure values. The total emission slowly but continuously decreases with increasing pressure. The intensity of the H(Lyα) emission line at low pressure is related to an increase in electron densities that enhance the production of H atoms. At higher pressure, the formation of H_2 by recombination of H atoms (in volume and on the wall), however, starts to overcome the production, leading to a decrease of H(Lyα) (Fozza et al. 1998). Moreover, with increasing gas pressure, non-radiative quenching processes of He* metastable species considerably reduce the H(Lyα) emission. Similar studies have been reported by Kurunczi et al. (2001), who studied a micro-hollow cathode plasma in He with the presence of H_2, O_2, and N_2 impurities and by Masoud et al. (2004) in the case of a cylindrical dielectric barrier discharge generated in a Ne/H_2 mixture. Besides quenching processes, the reduction of H(Lyα) emission at high pressure is also due to the radiation trapping as discussed by Woodworth et al. (2001), Masoud et al. (2004), and Titus et al. (2009).

Figure 5(b) shows the integrated emissions of H(Lyα) relative to the entire emission (i.e., 115–170 nm) as a function of the total pressure. Since at low pressure the total emission decreases more rapidly than H(Lyα) emission, the contribution of H(Lyα) goes through a maximum. The optimized conditions are thus reached when the total pressure is around 15 mbar, but the contribution of H(Lyα) is almost constant below 20 mbar.

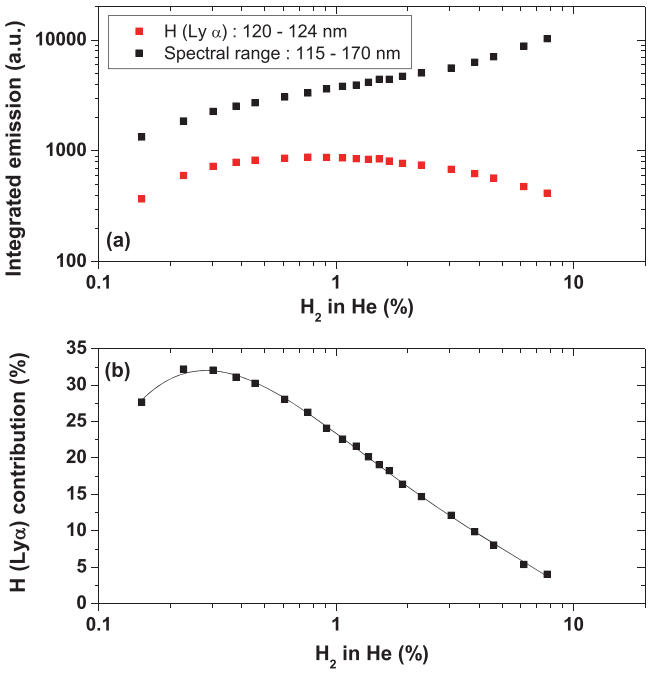

Figure 4. (a) Integrated emission of H(Lyα) in the range of 120–124 nm and total emission over 115–170 nm as a function of the H_2 concentration added in He. (b) The H(Lyα) contribution (normalized to the entire emission between 115 and 170 nm) as a function of the H_2percentage in He. For all measurements, the total pressure is constant at 4.7 mbar and the mean discharge power is 100 W. A polynomial fit has been added to the data to clarify the presentation.

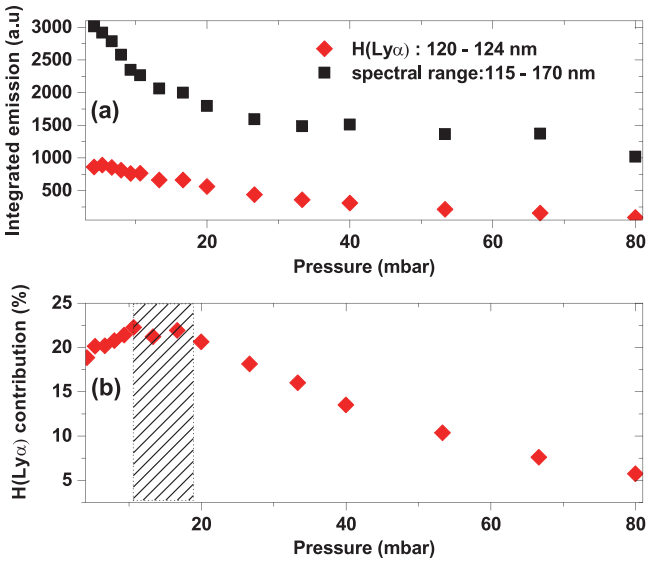

Figure 5. (a) Effect of the pressure on the integrated emission of H(Lyα) line between 120 and 124 nm, and total emissions in the range of 115–170 nm emitted from the microwave plasma in H_2/He mixtures. (b) Contribution of the integrated emission of H (Lyα) relative to the total integrated emission between 115 and 170 nm. The gray region is the optimum pressure conditions for the maximum contribution of H(Lyα) emission. For all the series of measurements, the H_2 amount added in He is kept at 1%. The partial flow rates of H_2 and He are 0.7 and 70 sccm, respectively. The mean discharge power is settled at 100 W.

3.1.4. Influence of the Flow Rate and Q/P Ratio

The role of the flow rate cannot be ignored in the characterization of the microwave plasma emission (Masoud et al. 2004). To study the contribution of H(Lyα), integrated between 120 and 124 nm relative to the spectral range over 115–170 nm, the most suitable parameter is the ratio (Q/p) between the flow rate and the measured pressure because of its correlation to the residence time of the gas inside the discharge tube (Es-sebbar et al. 2009). Flow rates between 2 and 40 sccm have been studied together with the gas pressure varying from 1 to 47 mbar. For all measurements, the percentage of H_2 in He was 2% and the power was settled at 100 W. Various values of Q/p were obtained by changing the pressure (p) for different flow rates (Q). Results shown in Figure 6 indicate that the relative contribution of H (Lyα) first increases with Q/p to reach a maximum and finally it decreases at high Q/p values. By increasing flow rates, the contribution of H(Lyα) rapidly decreases and the maximum is shifted to higher Q/p values. After reaching a maximum, the relative H(Lyα) contribution is independent on the Q/p parameter. Note that the optimum is always obtained for a pressure around 5 mbar. The flow rate should be kept as low as possible, and we thus recommend a flow rate of the order of 2 sccm, i.e., Q/p ratio of 0.4 sccm mbar^{-1}, to obtain the most monochromatic source. These observations can be explained by the role of the mean residence time in promoting H(Lyα) emission. The residence time is correlated to the Q/p parameter as well as the gas temperature (Es-sebbar et al. 2009). At short residence time (i.e., high Q/p values), the contribution of H(Lyα) increases when the residence time gets longer because H atom column density increases. However, further increase in the residence time (i.e., lower Q/p values) allows more H atom recombination, leading to a decrease in the H(Lyα) emission.

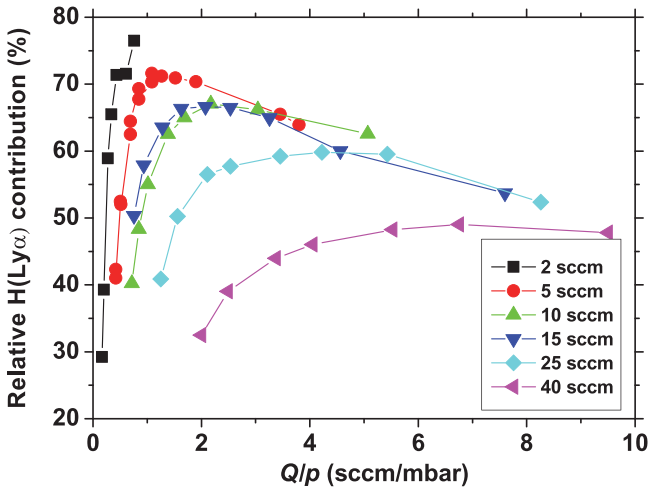

Figure 6. Contribution of the integrated emission of H(Lyα) relative to the total integrated emission between 115 and 170 nm. For all the series of measurements, the H_2 amount added to He was 2%. The parameter Q/p is determined by changing the pressure (p) for different flow rates (Q).

3.2. Chemical Actinometry, Irradiance, and Spectral Irradiance

To fully characterize our 1% H_2/He microwave-powered plasma light source, we have determined the VUV spectral irradiance (in ph cm^{-2} s^{-1} nm^{-1}) using chemical actinometry. Spectral irradiance is reported only in the range of 115–170 nm, the spectral domain extensively designed to mimic the solar radiation to study the photochemistry in astrophysical interests.

3.2.1. Chemical Actinometry

Chemical actinometry is a non-invasive diagnostic method that is easy to implement, which is generally used to determine the irradiance (in units of ph cm^{-2} s^{-1}). The irradiance of a lamp can be derived from the temporal production rate of a compound issued from the VUV photo-dissociation of an actinometer (Kuhn et al. 1989). Molecular oxygen (O_2), di-nitrogen oxide (N_2O), and carbon dioxide (CO_2) are commonly used since their photo-dissociation cross-sections in the VUV range are well known, as is the quantum yield of production of their photoproducts (O_3, NO, and CO, respectively). The advantage of CO_2 compared with O_2 or N_2O is that the formation of CO is taking place after a very short irradiation time (i.e., a few minutes; Romanzin et al. 2010). Therefore, we used CO_2 to derive the irradiance from the CO production rate (measured by FTIR spectroscopy) as a function of the irradiation time. If we assumed that the VUV photolysis is exclusively due to Lyα photons, the derivation of the irradiance is straight forward and has already been presented in details in Romanzin et al. (2010). This first method will be referred to here as the "monochromatic method."

In the present study, having previously measured the VUV spectrum of our 1% H_2/He microwave-powered lamp ($\Phi_\lambda^{\text{relative}}$), we have modified the equations reported by Romanzin et al. (2010) in order to take into account the CO_2 photolysis by any absorbed photons. We then used a new equation allowing us to determine the absolute spectral irradiance ($\Phi_\lambda^{\text{absolute}}$ in units of ph s^{-1} cm^{-2} nm^{-1}):

$$\Phi_\lambda^{\text{absolute}} = \frac{\Phi_\lambda^{\text{relative}}}{s}\frac{V}{L}\frac{dN\,(\text{CO})}{dt}\frac{1}{\int \Phi_\lambda^{\text{relative}}(\lambda)\eta_\lambda\varepsilon_\lambda d\lambda}, \quad (1)$$

where $dN\,(\text{CO})/dt$ is the temporal evolution of the CO column density during the photolysis (in molecules cm^{-2} s^{-1}), V is the volume of the infrared cell in which the CO_2 photolysis takes place ($V = (3042 \pm 3)\,cm^3$), L is the infrared path length ($L = 1040$ cm), and $\Phi_\lambda^{\text{relative}}$ is the emission spectrum of the lamp (in nm^{-1}) that has been previously normalized to 1 ($\int \Phi_\lambda^{\text{relative}}(\lambda)d\lambda = 1$). The parameter $S$is the area of the MgF_2 output windows of the lamp ($1\,cm^2$), and η_λ is the quantum yield of CO production from CO_2 photolysis, which is assumed to be equal to unity. The parameter ϵ_λ is the fraction of the photons flux absorbed by CO_2, which is given through the Beer–Lambert law:

$$\varepsilon_\lambda = 1 - \exp(\sigma_\lambda .\, l .\, p), \quad (2)$$

where σ_λ is the absorption cross section of CO_2 (in units of atm^{-1} cm^{-1}; Yoshino et al. 1996; Venot et al. 2013), l is the optical path length of the absorption cell, and p is the gas pressure of CO_2. The irradiance of the light source, $I_{\lambda1-\lambda2}^{\text{poly}}$ (in units of ph cm^{-2} s^{-1}) can be then calculated through the integration of the spectral irradiance:

$$\Phi_{\lambda1-\lambda2}^{\text{poly}} = \int_{\lambda1}^{\lambda2} \Phi_\lambda^{\text{absolute}}(\lambda)d\lambda. \quad (3)$$

Using this new method, the fact that the light source is polychromatic is taken into account for the first time. It is referred to here as the polychromatic method.

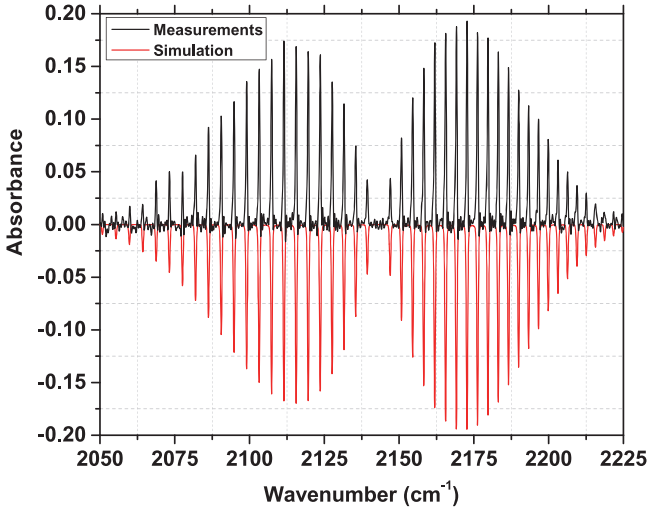

Figure 7. Comparison between experimental and calculated absorbance of CO issued from CO_2 after a photolysis time of 2520 s. The spectral resolution is 0.5 cm^{-1}. For clarity, the simulated absorbance is inverted.

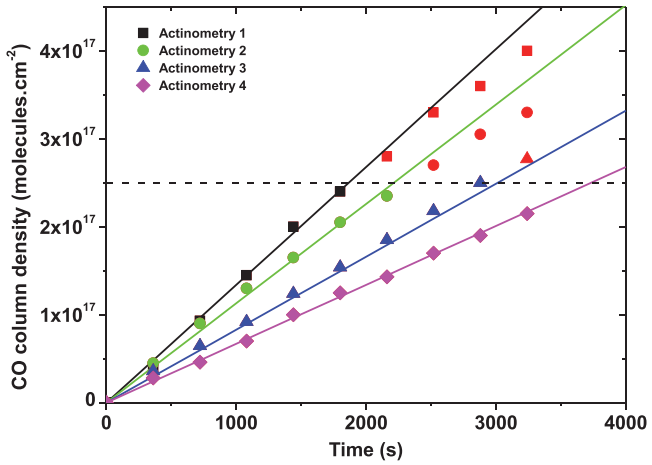

Figure 8. Time dependence of CO column density issued from four consecutive photolysis experiments of 0.8% CO_2 in N_2. The dotted line indicates the limit between the linear and the saturation region. The saturation appears for CO column densities higher than 2.5×10^{17} molecules cm^{-2} (red symbols). The time between each experiment is about one hour.

3.2.2. Absolute VUV Irradiance and Spectral Irradiance

Figure 7 compares the measured and calculated spectra of CO produced by dissociation of CO_2using our microwave-powered plasma. The synthetic spectra have been calculated using spectroscopic parameters taken from the GEISA database (Jacquinet-Husson et al. 2011). To avoid absorption saturation of the CO band, 0.8% of CO_2 was mixed with 1 bar of N_2. Line broadening due to molecular nitrogen ensures the linear dependence of the absorbance relative to column densities up to about 2.5×10^{17} cm^{-2}. Figure 8 presents the results of four experiments performed under the same experimental conditions with one-hour intervals using the following parameters: 1% H_2/He $p = 4.7$ mbar, 100 W, and flow rates of 0.7/70 sccm (H_2/He). Up to the saturation limit, a linear evolution of the CO column density is observed; thus, the slope value, $dN(\text{CO})/dt$ can be determined. The absolute VUV spectral irradiance $\Phi_\lambda^{\text{absolute}}$ can then be calculated using Equation (1). By comparing experiments 1 and 4, we observe

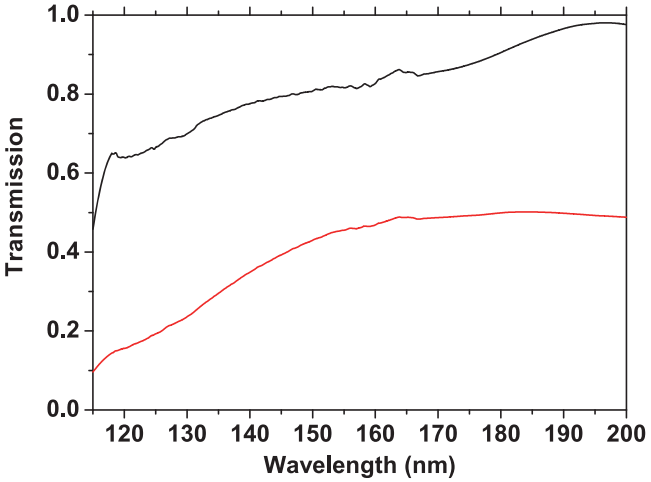

Figure 9. Transmission of the MgF_2 windows measured before (black) and after (red) eight hours of irradiation.

that the slopes decrease by about a factor of two, which is the result of a significant decrease of spectral irradiance over a lapse of time of a few hours. The corresponding irradiance integrated between 115 and 170 nm drops from 9.1 to 4.3×10^{14} ph s^{-1} cm^{-2} . This is related to the deposit of traces of species adsorbed on the MgF_2 window leading to a decrease of 50% of transmission after eight hours of irradiation experiments (Figure 9). A similar decrease of the transmission by more than one order of magnitude has already been observed by Warneck (1962) and Jenniskens et al. (1993). The nature of this deposit has not been found. Nevertheless, this deposit can be easily removed by cleaning the window with acetone and methanol solvents. The following measurements have been performed just after such cleaning.

In Table 2, the production rates of CO as a function of the microwave discharge power are reported, as well as irradiances calculated either with the "polychromatic" or the "monochromatic" method. Using the first approach, we have noted $I^{poly}_{115-124\,nm}$ and $I^{poly}_{115-170\,nm}$ irradiances calculated from the integration of the spectral irradiance $\Phi^{absolute}_{\lambda}$ between 115 and 124 nm and 115 and 170 nm, respectively. The results obtained with the second approach, noted as $I^{mono}_{Ly\alpha}$, are given for comparison.

From Table 2, one can note that an increase in the microwave power from 30 to 120 W leads to an increase by almost one order of magnitude of the CO production rates. A similar increase is observed for the $I^{poly}_{115-170\,nm}$ and $I^{mono}_{Ly\alpha}$ irradiances. Such an increase of irradiance with the microwave power has already been observed by Cottin et al. (2003). Moreover, the microwave power has an effect on the shape of the spectral irradiance $\Phi^{absolute}_{\lambda}$. Indeed, we observe that the H (Lyα) contribution is increased by a factor of four as shown by the ratio $I^{poly}_{115-124\,nm}$ versus $I^{poly}_{115-170\,nm}$. This is related to an increase in the average electron density that enhances the excitation rate of production of the hydrogen-excited species responsible for the VUV emissions. These considerations then have to be taken into account when microwave-powered lamps are used in photochemical studies, particularly when they are supposed to accurately simulate the VUV photons (mainly H (Lyα)) present in specific astrophysical interests (ISM or planetary environment). More importantly, the results of Table 2 show that the values of $I^{mono}_{Ly\alpha}$ are systematically overestimated by a factor of ~2.5 compared to the $I^{poly}_{115-170\,nm}$. This is later issued from a rigorous calculation using the "polychromatic method" that takes into account the entire spectrum of the lamp. In conclusion, we confirm that knowledge of the VUV emission spectrum is essential for determining accurate values of the irradiance of the lamp, which finally allows us to obtain quantitative data from the laboratory simulations.

4. DISCUSSION

4.1. Comparison with Previous VUV Irradiance

Table 3 shows quantitative measurements of photon flux (ph s^{-1}) or irradiance (ph s^{-1} cm^{-2}) performed on H_2(or mixtures of H_2 in noble gas) microwave-powered lamps used in various operating conditions in terms of pressure and microwave power. The current table is an updated version of the one published by Rajappan et al. (2010). With the exception of the present work and regardless of the actinometer used, the respective photons flux or irradiance have been determined using the "monochromatic method." As discussed in Section 3.2.2, this method leads to inaccurate values that are higher than the real output of the sources.

Results on lamps operating with mixtures of H_2 in He (Warneck 1962; Davis & Braun 1968) and in Ar (Okabe 1964;

Table 2
Effect of the Power on the Spectral Irradiance

Power (W)	$dN(CO)/dt$ (10^{14} molecules cm^{-2} s^{-1})	$I^{poly}_{115-124nm}$ (10^{14} ph cm^{-2} s^{-1})	$I^{poly}_{115-170nm}$ (10^{14} ph cm^{-2} s^{-1})	$\frac{I^{poly}_{115-124nm}}{I^{poly}_{115-170nm}}$ (%)	$I^{mono}_{Ly\alpha}$ (10^{14} ph cm^{-2} s^{-1})	$\frac{I^{mono}_{Ly\alpha}}{I^{poly}_{115-170nm}}$
30	0.19	0.08	1.15	7.0	3.10	2.7
40	0.345	0.163	2.10	7.8	5.63	2.7
50	0.5	0.29	3.09	9.4	8.17	2.6
60	0.655	0.481	4.10	11.7	10.7	2.6
80	0.88	0.956	5.68	16.8	14.4	2.5
100	1.38	1.93	9.15	21.1	22.5	2.5
120	1.58	2.76	10.8	25.5	25.8	2.4

Notes. The columns list the CO production rate and three different irradiances. The method of calculation differs between these three different values. $I^{poly}_{115-124\,nm}$ and $I^{poly}_{115-170\,nm}$ have been integrated from the spectral irradiances between 115 and 124 nm (H(Lyα)) and between 115 and 170 nm, respectively. $I^{mono}_{Ly\alpha}$ has been calculated using the "monochromatic method" (Romanzin et al. 2010), which assumed that all photons are emitted as H(Lyα) photons. Measurements have been performed under experimental conditions of 1%H_2/He gas, 4.7 mbar, and 0.7/70 sccm (H_2/He). Actinometry experiments are performed under 0.8% CO_2/N_2 (5.3/667 mbar).

Table 3
Photon Flux (ph s^{-1}) or Irradiance (ph cm^{-2} s^{-1}) Reported in the Literature Using Various Microwave-powered Sources and the Respective Method of Determination

Reference	Type of UV Lamp Gas/ Gas Mixture	Conditions: Pressure (mbar) and Power (W)	UV Spectrum	Method of Photon Irradiance Measurement	Photon Flux (10^{14} ph s^{-1}) * or Irradiance (10^{14} ph cm^{-2} s^{-1})**
Warneck (1962)	Flow lamp: 38% H_2 in He	0.2 mbar, 125 W	Relative Lyα and 160 nm	Photoelectric effect on Ni photocathode	20*
Okabe (1964)	Sealed off: 10% H_2 in Ar	1.33 mbar, 60 W	Relative Lyα	CO_2 actinometry	3*
Davis & Braun (1968)	Flow lamp: 2% H_2 in He	1.33 mbar, 125 W	No spectrum	CO_2 actinometry	7.6*
Yamashita (1975)	Plasma jet torch: 3.2% H_2 in Ar	6 mbar, 4000 W	Relative Lyα	#Thermal detector	20**
Hagen et al. (1979)	Flow lamp: Pure H_2	$(0.1–0.3) \times 10^{-1}$ mbar	Relative 160 nm	CO_2 actinometry	15*
Gerakines et al. (2000)	Flow lamp: Pure H_2	60–75 mbar, 50 W	No spectrum	O_2 photolysis	8.5**
Baratta et al. (2002)	Flow lamp: Pure H_2	Data not available	No spectrum	O_2 photolysis	(0.01–0.5)**,a
Cottin et al. (2003)	Flow lamp: Pure H_2	1333 mbar, 50 W	Relative Lyα and 160 nm	O_2 photolysis	5**,b
Rajappan et al. (2010)	Flow lamp: 10% H_2/Ar	1.33 mbar, 60 W	No spectrum	N_2O actinometry	10**
Romanzin et al. (2010)	Flow lamp: 2% H_2/He	4 mbar, 200 W	No spectrum	CO_2 actinometry	~62*
Cook et al. (2014)	Flow lamp: 0.68% H_2/He	1 mbar, 22–23 W	No spectrum	VUV-sensitive photodiode with sapphire window	$\sim 3.14 \times 10^{-3}$**
This work	Flow lamp: 1% H_2/He	4.7 mbar, 30–120 W	Absolute spectrum	CO_2 actinometry	(1.15–10.8)**

Notes. Results of the irradiance in the current work are presented in the last line, taking into account the polychromatic method.
[a] Irradiance is determined also with a platinium light detector.
[b] Irradiance is determined also with a NIST calibrated photodiode.

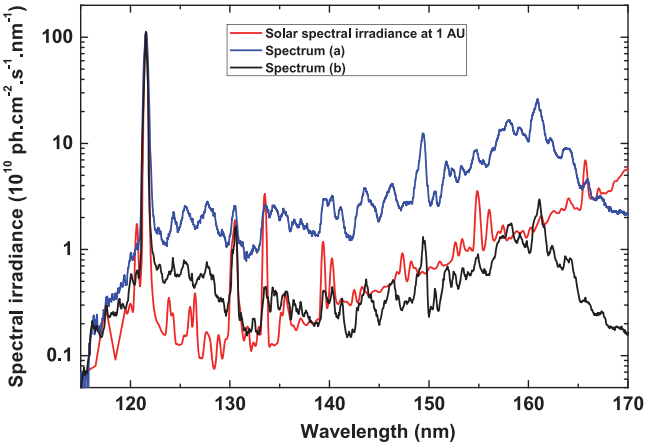

Figure 10. Spectral irradiances as a function of the wavelength. The red line is the solar irradiance at 1 AU, named "Atlas 3" (Thuillier et al. 2004). Spectrum (a), the blue line, is the spectral irradiance of our He/H_2 microwave lamp. This spectrum has been performed under experimental conditions of 1% H_2/He gas, 4.7 mbar, 70.7 sccm, and 100 W. The absolute spectral irradiance has been quantitatively determined by chemical actinometry and has been divided by 700 to scale the H(Lyα) emission line to the solar one. spectrum (b), the black line, is the spectrum of our lamp performed under experimental conditions of 2% H_2/He, 3 mbar, 5 sccm, and 100 W. This last spectrum has not been quantitatively measured by actinometry, so it is simply scaled to give the same Lyα intensity as the other two spectra.

Yamashita 1975) are reported. The only relative spectra of some of these lamps show either a contribution of both Lyα and 160 nm lines or an almost unique intense line at Lyα (Okabe 1964). As the light was produced by microwave excitation of different gas mixtures and under different operation conditions (static/flow, pressure, discharge power), the value of $I_{Ly\alpha}^{mono}$ was not the same, and furthermore, the actinometry method was different.

Such microwave-powered discharge lamps have been used in several experimental devices. For the study of the photolysis of interstellar grains, Hagen et al. (1979) reported a simulation of the UV flux in the ISM with a "frequently used to date" undiluted hydrogen flow lamp. Their spectrum presented a dominant emission near 160 nm. The photon flux, determined by CO_2actinometry, was found to be equal to 1.5 10^{15} ph s^{-1}. With the goal of understanding the photochemical evolution of interstellar/pre-cometary ice analogs, UV photolysis studies using a microwave discharge hydrogen lamp were reported in references (Jenniskens et al. 1993; Gerakines et al. 2000, 2004and references therein; Cottin et al. 2001, 2003; Baratta et al. 2002; Vuitton et al. 2006). They used the same device, but the operation experimental conditions (microwave power and H_2 pressure) were different. Moreover, the irradiance determined with the same actinometry method (i.e., O_2 photolysis) was found to vary from 8.6×10^{13} ph s^{-1} cm^{-2} (Gerakines et al. 2000) to 5×10^{14} ph s^{-1} cm^{-2} (Cottin et al. 2003). Experimental studies on methane photolysis at H(Lyα) were performed by Romanzin et al. (2010) using a 2% H_2/He lamp hoping to get a monochromatic emission as predicted by Davis & Braun (1968). The photon flux, determined by CO_2actinometry with the monochromatic method, turned out to be the highest ever achieved (6.2×10^{15} ph s^{-1}).

As pointed out by Chen et al. (2014), the spectrum of the lamp must be characterized accurately for astronomical laboratory studies of ice VUV photo processing. The parameters that can influence the spectrum and the irradiance of the lamps at H (Lyα) are (i) the gas mixture as already pointed out by Warneck (1962), (ii) the flow rate as demonstrated by Yamashita (1975), and (iii) the operating conditions of the microwave discharge as shown by the comparison of the spectrum and the irradiance of several pure H_2 (Opthos instrument) flow lamps (pressure and power). All these considerations have been confirmed and quantitatively assessed in the present work. The irradiances of our 1% H_2/He microwave-powered plasma source ranges from 1.15×10^{14} to 1.08×10^{15} ph s^{-1} cm^{-2}, depending on the microwave discharge power. These values are consistent with the data of the the literature.

4.2. Comparison with Solar VUV Spectral Irradiance

Figure 10 presents a comparison between the solar VUV spectral irradiance at 1 AU (Atlas 3 of Thuillier et al. 2004) with the emission spectrum of two microwave-powered lamps used in the present study. The first one has been acquired at a flow rate of 70 sccm and has been quantitatively calibrated by chemical actinometry. The spectral irradiance at H(Lyα) of our lamp is 700 times higher than the solar value, which allows us to study long timescale chemical processes. Nevertheless, with this large value for the gas flow rate, the contribution of H (Lyα) is quite low (see Figure 6), and it is lower than that of the solar one (see Figure 10). The second spectrum of Figure 10 was acquired with a total flow rate of 5 sccm and a pressure of 4 mbar, which corresponds to the maximum of the H(Lyα) contribution obtained in this study (see Figure 6). In that case, the shape of the solar spectra is well reproduced, and we can claim that our lamp, used under these conditions, is a good simulator of the solar spectra in the 115–170 nm range. Unfortunately, this last spectrum has not been calibrated by the chemical actinometry.

5. CONCLUSION

We have reported measurements of VUV emissions, photons flux, and spectral irradiance from microwave plasmas generated in H_2, He pure gases, and H_2/He mixture. In pure H_2, the mean feature emissions are H(Lyα) and a large Lyman band of H_2 ($B^1\Sigma_u$–$X^1\Sigma_g$). In pure He, the spectra are dominated by the impurity lines of H(Lyα), N, O, and C emissions rather than from energy transfer between the He* metastables and He_2* excimers with H_2, N_2, and O_2 impurities. In H_2/He microwave discharges, analysis of mean H (Lyα) and H_2 ($B^1\Sigma_u$–$X^1\Sigma_g$) spectral features has revealed a dependence on the H_2concentration. Even if the maximum H(Lyα) line emission over the entire spectrum in 115–170 nm is obtained around 0.3% H_2 in He, stable operation conditions for plasma sources to produce quasi-monochromatic VUV light were found in 1% H_2/He mixture at a pressure near 5 mbar and flow rate of 2 sccm (H_2/He). The chemical actinometry method using CO_2photolysis associated with FTIR spectroscopy has been used to measure the absolute spectral irradiance. Results were thoroughly compared to the available data in the literature and the solar spectrum. With appropriate operating conditions, the spectral irradiances of a H_2/He plasma and of the Sun have similar shape, while the absolute spectra irradiance of the laboratory plasma is higher than that of the Sun at 1 AU. A good agreement was obtained by comparing our photon flux with those used in laboratory experiments for simulating the energy deposition in planetary atmospheres and other

astrophysical media. Thus, this work significantly improves a detailed characterization of a microwave plasma source based on H_2 in terms of VUV flux and spectral irradiance. Our measurements provide a complete analysis of VUV photon flux. In planetary atmosphere and ISM laboratory simulation experiments, the control of the absolute VUV spectral irradiance is a crucial parameter. Therefore, the quantitative measurements presented in this article provide a new step that allows the optimization of the conditions used for microwave-powered lamps and finally achieves a better understanding of the chemistry in such environments.

We gratefully acknowledge the French Space Agency (Centre National d'Etudes Spatiales, CNES), the Ile de France Region (SESAME grant), and the French National Program of Planetary Sciences (PNP) for their financial support of the SETUP program. The authors gratefully acknowledge the CNES and the IPSL for their financial support in the frame of the EXPOSE International Space Station Program. E.E. thanks Université Paris Est Créteil (UPEC) for providing financial support.

REFERENCES

Baratta, G. A., Leto, G., & Palumbo, M. E. 2002, A&A, 384, 343
Chen, Y.-J., Chu, C.-C., Lin, Y.-C., et al. 2011, AdG, 25, 259
Chen, Y.-J., Chuang, K. J., Muñoz Caro, G. M., et al. 2014, ApJ, 781, 15
Cook, A. C., Mattioda, A. L., Quinn, R. C., et al. 2014, ApJS, 210, 15
Cottin, H., Moore, M. H., & Bénilan, Y. 2003, ApJ, 590, 874
Cottin, H., Szopa, C., & Moore, M. H. 2001, ApJL, 561, L139
Cruz-Diaz, G. A., Muñoz Caro, G. M., Chen, Y.-J., & Yih, T.-S. 2014, A&A, 562, A119
Davis, D., & Braun, W. 1968, ApOpt, 7/10, 2071
Ehrenfreund, P., Boogert, A. C. A., Gerakines, P. A., Tielens, A. G. G. M., & van Dishoeck, E. F. 1997, A&A, 328, 649
Es-sebbar, E., Benilan, Y., Jolly, A., & Gazeau, M.-C. 2009, JPhD, 42, 135206
Fedenev, A., Morozov, A., Kruchen, R., et al. 2004, JPhD, 37, 1586
Ferris, J., Tran, B., Joseph, J., et al. 2005, AdSpR, 36, 251
Fozza, A. C., Kruse, A., Holländer, A., Ricard, A., & Wertheimer, M. R. 1998, JVST, 16, 72
Fuchs, C., Goetzberger, O., Henck, R., & Fogarassy, E. 1995, APhA, 60, 505
Gazeau, M.-C., Cottin, H., Vuitton, V., Smith, N., & Raulin, F. 2000, P&SS, 48, 437
Gerakines, P. A., Moore, M. H., & Hudson, R. L. 2000, A&A, 357, 793
Gerakines, P. A., Moore, M. H., & Hudson, R. L. 2004, Icar, 170, 202
Hagen, W., Allamandola, L. J., & Greenberg, J. M. 1979, Ap&SS, 65, 215
Jacquinet-Husson, N., Crepeau, L., Armante, R., et al. 2011, JQSRT, 112, 2395
Jenniskens, P., Baratta, G. A., Kouchi, A., et al. 1993, A&A, 273, 583
Kuhn, H. J., Braslavsky, S. E., & Schmidt, R. 1989, PApCh, 61, 187
Kurunczi, P., Lopez, J., Shah, H., & Becker, K. 2001, IJMSp, 205, 277
Masoud, N., Martus, K., & Becker, K. 2004, IJMSp, 233, 395
Morozov, A., Heindl, T., Krücken, R., Ulrich, A., & Wieser, J. 2008, JAP, 103, 103301
Motret, O., Poversle, J. M., & Stevefelt, J. 1985, JChPh, 83, 1095
Muñoz Caro, G. M., & Schutte, W. A. 2003, A&A, 412, 121
Okabe, H. J. 1964, JOSA, 54, 478
Rajappan, M., Buttner, M., Cox, C., & Yates, J. T., Jr. 2010, JPCA, 114, 3443
Rahman, A., Yalin, A. P., Surla, V., et al. 2004, PSST, 13, 537
Romanzin, C., Arzoumanian, E., Es-sebbar, E., et al. 2010, P&SS, 58, 1748
Samson, J. A. R. 1967, in Techniques of Vacuum Ultraviolet Spectroscopy (Lincoln, NE: Pied Publications)
Titus, M. J., Nest, D., & Graves, D. B. 2009, ApPhL, 94, 171501
Tran, B., Force, M., Briggs, R. G., et al. 2008, Icar, 193, 224
Thuillier, G., Floyd, L., Woods, T. N., et al. 2004, AdSpR, 34, 256
Venot, O. N., Fray, Y., Benilan, M.-C., et al. 2013, A&A, 551, A131
Vuitton, V., Doussin, J.-F., Bénilan, Y., Raulin, F., & Gazeau, M.-C. 2006, Icar, 185, 287
Warneck, P. 1962, ApOpt, 1, 721
Weber, P., & Greenberg, J. M. 1985, Natur, 316, 403
Woodworth, J. R., Riley, M. E., Amatucci, V. A., Hamilton, T. W., & Aragon, B. P. 2001, JVST, 19, 45
Yamashita, I. 1975, JaJAP, 14, 70
Yoshino, K., Esmond, J. R., Sun, Y., et al. 1996, JQSRT, 55, 53